PHYSICAL REVIEW A **73**, 064701 (2006)

Applicability of modified effective-range theory to positron-atom and positron-molecule scattering

Zbigniew Idziaszek

CNR-INFM BEC Center, I-38050 Povo, Italy and Centrum Fizyki Teoretycznej, Polska Akademia Nauk, 02-668 Warsaw, Poland

Grzegorz Karwasz

Instytut Fizyki, Uniwersytet Mikołaja Kopernika, 87-100 Toruń, Poland

We analyze low-energy scattering of positrons on Ar atoms and N_2 molecules using the modified effective-range theory (MERT) developed by O'Malley, *et al.* [J. Math. Phys. **2**, 491 (1961)]. We use the formulation of MERT based on exact solutions of the Schrödinger equation with polarization potential rather than low-energy expansions of phase shifts into momentum series. We show that MERT describes the experimental data well, provided that effective-range expansion is performed both for *s*- and *p*-wave scattering, which dominate in the considered regime of positron energies (0.4–2 eV). We estimate the values of the *s*-wave scattering length and the effective range for e^+-Ar and e^+-N_2 collisions.

PACS number(s): 34.85.+x

Electron (and positron) scattering on atoms at very low energies is dominated by polarization forces. The modified effective range theory (MERT) was developed by O'Malley *et al.* [1,2] for low-energy scattering of charged particles on neutral polarizable systems in general. O'Malley [3] applied MERT for electron scattering on noble gases, in particular in the region of Ramsauer-Townsend minimum, using early total [4] and momentum transfer [5] experimental cross sections. Haddad and O'Malley [6] used a three-parameter MERT fit for *s*-wave phase shift in electron-argon scattering and Ferch *et al.* [7]—for Ramsauer minimum in methane. Higher-order terms in MERT, resulting from short-range components of polarizability, were introduced by Ali and Fraser [8]. MERT analysis for Ne, Ar, and Kr up to 1 eV was carefully revisited by Buckman and Mitroy [9] who used a five-parameter fit for *s*-wave and *p*-wave shifts.

Applicability of MERT to low-energy positron scattering was already hypothesized in [2]. However, first measurements of total cross sections for positron scattering at low energies on noble atoms come only from seventies [10,11].

The most systematic data for noble atoms, extending down to 0.3 eV were done in Wayne State University Detroit Lab, using positrons from a short-lived C^{11} radionuclid, with about 0.1 eV energy resolution [11]. Those data clearly indicated a rise in the cross section in the zero-energy limit in gases, such as He, Ar, H_2, Kr, Xe, and CO_2, see [11]. Unfortunately, subsequent experiments [12,13] used a Ne^{22} source and a thick W-vanes positron moderator, thus worsening the energy resolution and not allowing reliable measurements below 1 eV. To gain in signal, large apertures and strong guiding magnetic fields were used, leading to an underestimation of cross sections—some data even showed a fall in the limit of zero energy for highly polarizable targets, such as C_6H_6 [14].

Only two of the most recent setups reached energies below 1 eV with a good signal-to-noise ratio. In San Diego, annihilation rates in Ar and Xe were measured which showed a steep rise below 1 eV [15]. In Trento, total cross sections in Ar and N_2 were measured [16] with angular resolution better

by a factor of 30 than in some previous experiments [12]. Both laboratories confirm the early observations from WSU Detroit on the rise of positron cross sections in the zero-energy limit. Such a rise is also predicted by *ab initio* theories [17], see [16] for a detailed comparison. A phenomenological attempt to apply a MERT-like fit for low-energy cross sections in benzene and cyclohexane was done by Karwasz *et al.* [18].

In the present paper, we apply MERT to positron total cross sections on argon and nitrogen, using recent experimental data from Trento [16]. We use the MERT model based on the direct solution of the Schrödinger equation with a polarization potential as originally proposed by O'Malley *et al.* [1]. Different from earlier works, for the *p*-wave phase shift, we consider not only the polarization potential but the contribution from a general-type short-range interaction. This allows us to extend the MERT applicability for positrons to energies above 1 eV. A clear indication on the importance of *p*-wave scattering in this energy range comes from recent differential cross sections measurements in argon [19]. The present model introduces a second MERT parameter for the *p*-wave shift thus developing an approximation with two parameters for both the *s*- and *p*-wave phaseshifts. The first parameter is to be interpreted as a scattering length, and the second as an effective range. We compare our MERT model with the expansion into the momentum series valid at low energies and with *ab initio* theories [17,20].

Let us briefly review the effective-range expansion for $1/r^4$ interaction. We divide the interaction potential between a charged particle and a neutral atom into the long-range part: $V_p(r) = -\alpha e^2/(2r^4)$ with α denoting the atomic polarizability and e as the charge, and the short-range part: $V_s(r)$ describing forces acting at distances comparable to the size of atoms. In the relative coordinate, the motion of particles is governed by

$$\left[\frac{\partial^2}{\partial r^2} + \frac{2}{r}\frac{\partial}{\partial r} - \frac{l(l+1)}{r^2} + \frac{(R^*)^2}{r^4} + k^2 \right] \Psi(r) = 0, \quad (1)$$

where $\Psi(r)$ denotes the radial wave function for *l*th partial wave, $\hbar k$ is the relative momentum of the particles, R^*

$\equiv \sqrt{\alpha e^2 \mu / \hbar^2}$ denotes a typical length scale related to the r^{-4} interaction, and μ denotes the reduced mass. In Eq. (1), we do not include $V_s(r)$, which is replaced by appropriate boundary condition at $r \to 0$. The Schrödinger equation with polarization potential can be solved analytically [1,21,22] (see Appendix for details). At small distances ($r \ll R^*$), behavior of $\Psi(r)$ is governed by

$$\Psi(r) \overset{r \to 0}{\sim} \sin\left(\frac{R^*}{r} + \phi\right), \qquad (2)$$

where ϕ is a parameter which is determined by the short-range part of the interaction potential. For $r \gg R^*$, $\Psi(r)$ takes the form of the scattered wave

$$\Psi(r) \overset{r \to \infty}{\sim} \frac{1}{kr} \sin\left(kr - l\frac{\pi}{2} + \eta_l\right), \qquad (3)$$

with the phase shift η_l

$$\tan \eta_l = \frac{m^2 - \tan \delta^2 + B \tan \delta(m^2 - 1)}{\tan \delta(1 - m^2) + B(1 - m^2 \tan^2 \delta)}, \qquad (4)$$

where we use a similar notation as in Ref. [1]. Here, $B = \tan(\phi + l\pi/2)$, $\delta = \pi/2(\nu - l - 1/2)$, and m and ν are parameters obtained from the analytic solution of the Mathieu's differential equation (see Appendix). To introduce the effective range, we expand B around zero energy: $B(k) = B(0) + 1/2R_0 R^* k^2 + \ldots$ [1]. The second term can be interpeted as a correction due to the finite range of the interaction, with R_0 representing the effective range.

In the zero-energy limit, expansion of MERT in series of momentum k is useful. In the particular case of $l=0$, $B(0)$ can be expressed in terms of s-wave scattering length a_s: $B(0) = -R^*/a_s$, and expansion of $\cot \eta_0$ at $k=0$ yields [1,23]

$$q \cot \eta_0(q) = -\frac{1}{a} + \frac{\pi}{3a^2}q + \frac{4}{3a}\ln\left(\frac{q}{4}\right)q^2 + \frac{R_0^2}{2(R^*)^2}q^2$$
$$+ \left[\frac{\pi}{3} + \frac{20}{9a} - \frac{\pi}{3a^2} - \frac{\pi^2}{9a^3} - \frac{8}{3a}\psi\left(\frac{3}{2}\right)\right]q^2 + \ldots \qquad (5)$$

where $a = a_s/R^*$, $q = kR^*$ and $\psi(3/2)$ denotes the digamma function [24]. We apply similar procedure for the p wave. In this case, however, we expand directly $\tan \eta_1$ given by Eq. (4)

$$\tan \eta_1 = \frac{\pi q^2}{15} + \frac{q^3}{9b} - \frac{83\pi q^4}{23625} - \frac{4}{135b}\ln\left(\frac{q}{4}\right)q^5 - \frac{R_1}{18b^2 R^*}q^5$$
$$+ \frac{15\pi - 15\pi b^2 - 148b + 120b\psi\left(\frac{5}{2}\right)}{2025b^2}q^5 + \ldots \qquad (6)$$

Here, $b = B(0)$ for $l=1$, and R_1 denotes the effective range for the p wave. For higher partial waves, we retain only the lowest-order term in k, which is sufficient to describe the scattering in the considered regime of energies

$$\tan \eta_l \approx -\frac{\pi q^2}{8(l-1/2)(l+1/2)(l+3/2)}, \quad l \geq 2. \qquad (7)$$

TABLE I. Characteristic distance R^*, characteristic energy E^*, and four fitting parameters: a_s (s-wave scattering length), R_0 (s-wave effective range), b [zero-energy contribution B(0) for p-wave] and R_1 (p-wave effective range) for Ar and N_2.

	$R^*(a_0)$	E^*(eV)	a_s/R^*	b	R_0/R^*	R_1/R^*
Ar	3.351	1.211	−1.665	−5.138	0.3165	2.281
N_2	3.397	1.179	−2.729	−12.65	0.8186	—

Let us turn now to positron scattering. We compare the total cross section measured in experiments for Ar and N_2 [16] with predictions of the theoretical model based on the effective-range expansion. In our approach, the effects of the short-range potential are included both for the s and p waves giving the leading contribution to the scattering in the considered regime of energies. Thus, our model contains four unknown parameters: The scattering length a and the effective range R_0 for the s wave, and the zero-energy contribution $b = B(0)$ and the effective range R_1 for a p wave. For the investigated regime of positrons energies, $q = kR^*$ can take values larger than unity, therefore for s and p waves, we do not use expansions (5) and (6) valid for $q \lesssim 1$, but rather, we applied the initial formula (4) for the phase shift, performing only finite-range expansion for the parameter B. In this case, values of ν and m have to be evaluated numerically, using the approach described in the Appendix.

For the calculations, we use recent experimental values of the polarizability: $\alpha = 11.23a_0^3$ and $\alpha = 11.54a_0^3$ (atomic units), for Ar and N_2, respectively [25]. Table I contains values of the characteristic distance R^* and the characteristic energy $E^* = \hbar^2/(2\mu R^{*2})$ for the polarization potential, and the values of four parameters: a, b, R_0, and R_1 which were determined by fitting our model to the experimental data.

In the case of N_2, the size of the molecule scaled by R^* is much larger than for Ar, therefore we restricted our effective-range analysis to lower energies, fitting the model to experimental data with $E \lesssim 0.8E^*$. In this regime, the contribution of the effective-range correction in the p wave is rather small, and one does not get reliable results for this parameter from the fitting procedure. Thus, for N_2, we considered only three parameters—a, b, and R_0—accounting for the effects of the short-range part of the potential.

Figure 1 shows the experimental data for the total scattering cross section for Ar as a function of positron collision energy. They are compared with: The MERT theoretical curve which best fits the experimental data, its low-energy expansion given by Eqs. (5)–(7), and the results of McEachran *et al.* [17]. The total cross section is presented in units of R^*, while the energy is scaled by E^*. In the inset, we additionally present contributions of the s and p waves to the total scattering cross section. Similar results, except for the scattering of positrons on N_2, are illustrated in Fig. 2.

We note the good agreement between our model and the results of McEachran *et al.* [17] at low energies. The obtained value of the scattering length $a_s = -5.58a_0$ agrees well with the calculations of McEachran *et al.* [17] $(-5.30a_0)$, and Nakanishi and Schrader [20] $(-5.09a_0)$. A somewhat worse agreement in N_2 can partially result from poorer statistics of
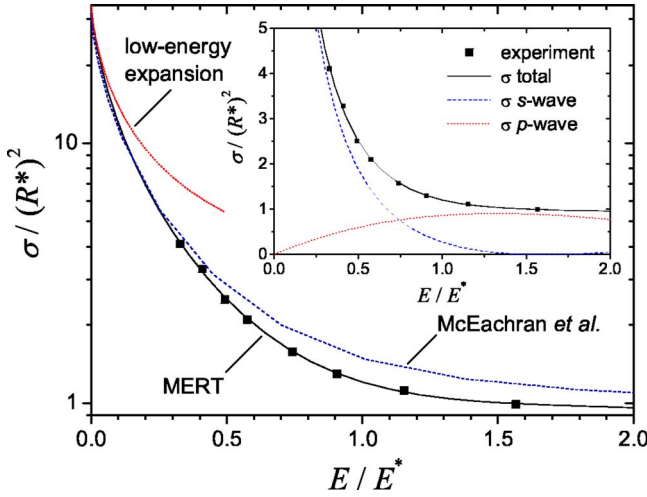
FIG. 1. (Color online) Total cross section for the scattering of positrons on argon versus the energy. Depicted are: Experimental data (squares), the theoretical fit based on effective-range expansion (solid line), its low-energy part given by Eqs. (5)–(7), and the theoretical results of McEachran *et al.* [17] (dashed line). The inset shows in addition the *s*- and *p*-wave cross-sections. Data are scaled by the characteristic distance R^* and the characteristic energy E^* of the polarization potential.

experimental data. Also ab-initio theoretical calculation in N_2 show a big spread in determination of a_s, see for instance [26]. Both for Ar and N_2 the model shows importance of *p*-wave scattering above 0.7–0.8 eV. The *s*-wave effective range for Ar amounts to $1.06a_0$ while in N_2 to $2.78a_0$. We recall the "size" of the N_2 molecule by the experimental determination of the maximum highest occupied molecular orbital density along the molecule axis which is about $2.3a_0$ [27]. Finally from Figs. 1 and 2, we observe that expansion into momentum series (5)–(7) works only at very low energies below 0.1 eV.

In conclusion, we performed MERT analysis using an analytical solution of the Schrödinger equation for polarization potential, and we apply it to positron Ar (and N_2) scat-
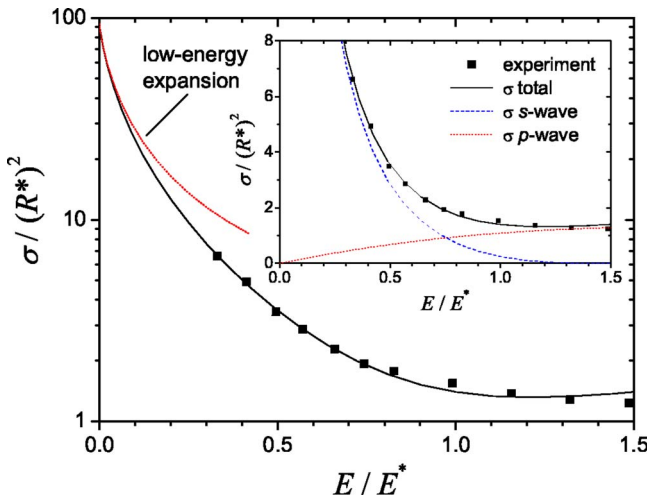

FIG. 2. (Color online) The same as Fig. 1, but for the scattering of positrons on N_2.

tering up to 2 eV. The scattering length in Ar agrees well with other predictions and the effective range (for the *s* wave) is $1.06a_0$. More experiments are needed at low energies to better validate the effective range parameters.

APPENDIX

To solve radial Schrödinger equation (1), we substitute $r = \sqrt{R^*e^{-z}}/\sqrt{k}$ and $\Psi(r) = \psi(r)\sqrt{R^*/r}$, which yields the Mathieu's modified differential equation [24,28]

$$\frac{d^2\psi}{dz^2} - [a - 2q\cosh 2z]\psi = 0. \tag{A1}$$

where $a = (l+1/2)^2$ and $q = kR^*$. Two linearly indepent solutions $M(z)$ and $T(z)$ can be expressed in the following form [22,28]:

$$M_\nu(z) = \sum_{n=-\infty}^{\infty} (-1)^n c_n(\nu) J_{2n+\nu}(2\sqrt{q}\cosh z), \tag{A2}$$

$$T_\nu(z) = \sum_{n=-\infty}^{\infty} (-1)^n c_n(\nu) Y_{2n+\nu}(2\sqrt{q}\cosh z), \tag{A3}$$

which defines them for $z > 0$. Here, ν denotes the characteristic exponent, and $J_\nu(z)$ and $Y_\nu(z)$ are Bessel and Neumann functions, respectively. Substituting the ansatz (A2) and (A3) into Eq. (A1), one obtains the recurrence relation:

$$[(2n+\nu)^2 - a]c_n + q(c_{n-1} + c_{n+1}) = 0, \tag{A4}$$

which can be solved in terms of continued fractions. To this end, we introduce $h_n^+ = c_n/c_{n-1}$ and $h_n^- = c_{-n}/c_{-n+1}$ for $n > 0$, which substituted into Eq. (A4) gives the continued fractions $h_n^+ = -q/(qh_{n+1}^+ + d_n)$, and $h_n^+ = -q/(qh_{n+1}^+ + d_n)$ with $d_n = (2n+\nu)^2 - a$. In practice, to find numerical values of the coefficients c_n, we set $h_m^+ = 0$ and $h_m^- = 0$ for some sufficiently large m and calculate h_n^+ and h_n^- up to $n=1$. The characteristic exponent has to determined from Eq. (A4) with $n=0$.

Asymptotic behaviors of $M_\nu(z)$ and $T_\nu(z)$ for large z immediately follow from the asymptotic expansion of Bessel functions

$$M_\nu(z) \xrightarrow{z \to \infty} \sqrt{\frac{2}{\pi}} \frac{e^{-z/2}}{q^{1/4}} s_\nu \cos\left(e^z\sqrt{q} - \frac{\pi}{2}\nu - \frac{\pi}{4}\right), \tag{A5}$$

$$T_\nu(z) \xrightarrow{z \to \infty} \sqrt{\frac{2}{\pi}} \frac{e^{-z/2}}{q^{1/4}} s_\nu \sin\left(e^z\sqrt{q} - \frac{\pi}{2}\nu - \frac{\pi}{4}\right), \tag{A6}$$

where $s_\nu = \Sigma_{n=-\infty}^{\infty} c_n(\nu)$. To obtain asymptotic behaviors for large and negative z, one has to join solutions $M_\nu(z)$ and $T_\nu(z)$, with another pair of solutions $M_\nu(-z)$ and $T_\nu(-z)$ at $z=0$ [22]. This yields

$$M_\nu(z) \xrightarrow{z \to -\infty} \sqrt{\frac{2}{\pi}} \frac{e^{z/2}}{q^{1/4}} m s_\nu \cos\left(\sqrt{q}e^{-z} + \frac{\pi}{2}\nu - \frac{\pi}{4}\right), \tag{A7}$$

$$T_\nu(z) \xrightarrow{z \to -\infty} -\sqrt{\frac{2}{\pi}} \frac{e^{z/2}}{q^{1/4}} \frac{s_\nu}{m} \left[\sin\left(\sqrt{q} e^{-z} + \frac{\pi}{2}\nu - \frac{\pi}{4} \right) \right.$$
$$\left. - \cot \pi\nu (m^2 - 1)\cos\left(\sqrt{q} e^{-z} + \frac{\pi}{2}\nu - \frac{\pi}{4} \right) \right],$$
$$\text{(A8)}$$

where $m = \lim_{z \to 0^+} M_\nu(z)/M_{-\nu}(z)$.

Finally, we write the wave function $\Psi(r)$ in the form

$$\Psi(r) = \sin\left(\phi + \frac{\pi}{2}\nu + \frac{\pi}{4} \right) \sqrt{\frac{R^*}{r}} M_\nu\left(\ln \frac{\sqrt{R^*}}{\sqrt{kr}} \right)$$
$$+ \cos\left(\phi + \frac{\pi}{2}\nu + \frac{\pi}{4} \right) \sqrt{\frac{R^*}{r}} T_\nu\left(\ln \frac{\sqrt{R^*}}{\sqrt{kr}} \right), \quad \text{(A9)}$$

where ϕ is a parameter which appears in the small r expansion (2). Now, the behavior of $\Psi(r)$ at small and large distances described by Eqs. (2)–(4), can be readily obtained from asymptotic expansions (A5)–(A8).

---

[1] T. F. O'Malley, L. Spruch, and L. Rosenberg, J. Math. Phys. **2**, 491 (1961).

[2] T. F. O'Malley, L. Rosenberg, and L. Spruch, Phys. Rev. **125**, 1300 (1962).

[3] T. F. O'Malley, Phys. Rev. **130**, 1020 (1963).

[4] C. Ramsauer and Kollath, Ann. Phys. **3**, 536 (1929).

[5] J. L. Pack and A. V. Phelps, Phys. Rev. **121**, 798 (1961).

[6] G. N. Haddad and T. F. O'Malley, Aust. J. Phys. **35**, 35 (1982); T. F. O'Malley and R. W. Crompton, J. Phys. B **13**, 3451 (1980).

[7] J. Ferch, G. Granitza, and W. Raith, J. Phys. B **18**, L445 (1985).

[8] M. K. Ali and P. A. Fraser, J. Phys. B **10**, 3091 (1977).

[9] S. J. Buckman and J. Mitroy, J. Phys. B **22**, 1365 (1989).

[10] D. G. Costello, D. E. Groce, D. F. Herring, and J. Wm. McGowan, Can. J. Phys. **50**, 23 (1972).

[11] W. E. Kauppila, T. S. Stein, and G. Jesion, Phys. Rev. Lett. **36**, 580 (1976); see also, W. E. Kauppila and S. T. Stein, Adv. At., Mol., Opt. Phys. **26**, 1 (1990).

[12] O. Sueoka and S. Mori, J. Phys. Soc. Jpn. **53**, 2491 (1984).

[13] T. S. Stein, W. E. Kauppila, C. K. Kwan, S. P. Parikh, and S. Zhou, Hyperfine Interact. **73**, 53 (1992).

[14] M. Kimura, C. Makochekanwa, and O. Sueoka, J. Phys. B **37**, 1461 (2004).

[15] J. P. Marler, L. D. Barnes, S. J. Gilbert, J. P. Sullivan, J. A. Young, and C. M. Surko, Nucl. Instrum. Methods Phys. Res. B **221**, 84 (2004).

[16] G. P. Karwasz, D. Pliszka, and R. S. Brusa, Nucl. Instrum. Methods Phys. Res. B, **247**, 68 (2006), see also, G. P. Karwasz, Eur. Phys. J. D **35**, 267 (2005).

[17] R. P. McEachran, A. G. Ryman, and A. D. Stauffer, J. Phys. B **12**, 1031 (1979).

[18] G. Karwasz, D. Pliszka, and A. Zecca, Proc. SPIE **5849**, 243 (2005).

[19] J. P. Sullivan, S. J. Gilbert, J. P. Marler, R. G. Greaves, S. J. Buckman, and C. M. Surko, Phys. Rev. A **66**, 042708 (2002).

[20] H. Nakanishi and D. M. Schrader, Phys. Rev. A **34**, 1823 (1986).

[21] E. Vogt and G. H. Wannier, Phys. Rev. **95**, 1190 (1954).

[22] R. M. Spector, J. Math. Phys. **5**, 1185 (1964).

[23] B. R. Levy and J. B. Keller, J. Math. Phys. **4**, 54 (1963).

[24] M. Abramowitz and I. A. Stegun, *Handbook of Mathematical Functions* (Dover, New York, 1972).

[25] T. N. Olney, N. M. Cann, G. Cooper, and C. E. Brion, Chem. Phys. **223**, 59 (1997).

[26] F. A. Gianturco, P. Paioletti, and J. A. Rodriguez-Ruiz, Z. Phys. D: At., Mol. Clusters **36**, 51 (1996).

[27] J. Itatani, J. Levesue, D. Zeidler, H. Niikura, H. Ppin, J. C. Kieffer, P. B. Korkum, and D. M. Villeneuve, Nature (London) **432**, 867 (2004).

[28] A. Erdélyi, *Higher Transcendental Functions* (McGraw–Hill, New York, 1955), Vol. 3.